2.D

ANGULAR MOMENTUM EFFECTS
IN THE COMPOUND-STATISTICAL MODEL FOR NUCLEAR REACTIONS
(I). Monte Carlo calculations of excitation functions

D. G. SARANTITES and B. D. PATE [†]

Department of Chemistry, Washington University, St. Louis, Missouri [††]

Abstract: The evaporation formalism of the compound-statistical theory of nuclear reactions is presented in a form containing the explicit dependence of the emission probability on angular momentum and suitable for computation of excitation functions by the Monte Carlo technique. The dependence of the nuclear level density on angular momentum is discussed, and an improved expression is offered. Monte Carlo calculations have led to the evaluation of excitation functions in selected reactions and the results were compared with experiment. The effect of competing de-excitation by gamma-ray emission is examined and its magnitude is estimated from an analysis of excitation function data. Satisfactory agreement between calculated and experimental excitation functions induced by ^{4}He ions of kinetic energy up to 40 MeV is obtained using the Fermi gas model parameters for the level density expression.

1. Introduction

There are three types of nuclear reaction data, namely, excitation functions, particle evaporation spectra and nuclear isomer yield ratios, which have been analysed on the basis of the compound-statistical model [1-5]. Such analyses of excitation function data [6-12] led to values for the level density parameter a appreciably smaller than predicted by the Fermi gas model. Analyses of experimental nuclear evaporation spectra [13, 14], on the other hand, resulted in decreasing a-values with increasing projectile energy even when angular momentum effects were approximately taken into account. Finally data on isomer yield ratios [15, 16] were best reproduced with a-values appreciably higher than those obtained from particle spectra. Attempts to include angular momentum effects in an approximate way into calculations of excitation functions where one or more particles are evaporated have been made recently by several authors [17-23].

In this paper a formalism of the compound-statistical model is presented which is suitable for simultaneous calculation of excitation functions, particle evaporation spectra and isomer yield ratios in reactions involving the evaporation of one or more

particles. The formalism explicitly includes the dependence of the emission probability on angular momentum. In this work the Monte Carlo technique has been adopted because it leads to a computationally simple formalism.

2. Formalism

The cross section for a nuclear reaction induced by a projectile b of energy ε_b on a target T in the formalism of the compound-statistical model can be expressed as a product of two factors, i.e. (i) the cross section for the formation of a compound nucleus with excitation energy U and angular momentum and parity $J_c \pi_c$ and (ii) the probability that this compound nucleus will decay to a product nucleus with residual energy E_f and angular momentum and parity $J_f \pi_f$. Thus the total cross section for the observed reaction can be written as the sum of the cross sections of the possible paths as follows:

$$\sigma(b, x) = \sum_{J_c \pi_c} \sigma_{comp}^b(U, J_c^k) \frac{\Gamma_x(U, J_c)}{\sum_i \Gamma_i(U, J_c)}, \tag{1}$$

where b stands for the parameters of the incoming channel, namely, J_t^i the spin and parity of the target, ε_b the projectile energy and s_b the projectile spin. The cross section $\sigma_{comp}^b(U, J_c^k)$, usually called the capture cross section, when summed over J_c^k gives the absorption cross section $\sigma_b(\varepsilon_b)$ of the optical model for the channel b. If the spin-orbit interaction energy in the optical potential is neglected then the "channel-spin" coupling scheme gives for the capture cross section

$$\sigma_{comp}^b(U, J_c^k) = \pi \lambda^2 \frac{(2J_c^k + 1)}{(2s_b + 1)(2J_t^i + 1)} \left[\sum_{I = |J_t^i - s_b|}^{J_t^i + s_b} \sum_{l = |J_c^k - I|}^{J_c^k + I} \pi(l) T_l(\varepsilon_b) \right], \tag{2}$$

where I is the so-called channel spin and λ the de-Broglie wave length for the projectile in the centre-of-mass system; $\pi(l)$ is zero for odd l, if there is no parity change and for even l if there is parity change between the initial and the final state, $T_l(\varepsilon_b)$ is the transmission coefficient for the lth incident partial wave, ε_b the kinetic energy of the incoming particle and the superscript of J_t or J_c the parity of the state.

If the spin-orbit interaction is included in the optical-model potential then the j-j coupling scheme for s_b equal to $\frac{1}{2}$ gives (see appendix 1)

$$\sigma_{comp}^b(U, J_c^k) = \pi \lambda^2 \frac{(2J_c^k + 1)}{2(2J_t^i + 1)}$$

$$\times \left[\sum_{l = |J_c^k - J_t^i \pm \frac{1}{2}|}^{J_c^k + J_t^i + \frac{1}{2}} \pi(l) T_l^{j = l - \frac{1}{2}}(\varepsilon_b) + \sum_{l = |J_c^k - J_t^i \mp \frac{1}{2}|}^{J_c^k + J_t^i - \frac{1}{2}} {\{}^{\text{for } J_c^k > J_t^i}_{\text{for } J_c^k < J_t^i} \pi(l) T_l^{j = l + \frac{1}{2}}(\varepsilon_b) \right], \tag{3}$$

where now $T_l^{j = l \pm \frac{1}{2}}(\varepsilon_b)$ stands for the transmission coefficient of the lth partial wave with the projectile spin parallel or antiparallel to l. The signs in the lower summation

limits are to be selected according to whether $J_c > J_t$ or $J_c < J_t$ as indicated. In expressions (2) and (3) parity selection rules would be ignored if one substitutes unity for $\pi(l)$.

As yet there is no definite experimental evidence in support of one of the above coupling schemes, but the "channel-spin" scheme has been widely used. The difference in (2) and (3) is more pronounced in reactions induced by medium- or low-energy neutrons and protons on targets of low spin. At higher energies and/or in targets with high spin values, the spin-orbit interaction effects on the transmission coefficients are of minor importance and (2) and (3) give approximately the same result.

The optical-model absorption cross section or the total reaction cross section $\sigma_b(\varepsilon_b)$ is simply the sum of (2) or (3) over all $J_c\pi_c$, that is, from 0 or $\tfrac{1}{2}$ to "infinity". Actually, the summation should be extended up to the maximum value J_c which can be populated. Carrying out this summation over J_c up to "infinity" one finds the following expressions from (2) or (3), respectively,

$$\sigma_b(\varepsilon_b) = \pi\lambda^2 \sum_{l=0}^{\infty} (2l+1)T_l(\varepsilon_b), \tag{4}$$

$$\sigma_b(\varepsilon_b) = \pi\lambda^2 \sum_{l=0}^{\infty} [(l+1)T_l^{j=l+\frac{1}{2}}(\varepsilon_b)+lT_l^{j=l-\frac{1}{2}}(\varepsilon_b)]. \tag{5}$$

Average transmission coefficients $T_l(\varepsilon_b)$ could be defined by

$$T_l(\varepsilon_b) = \frac{l+1}{2l+1} T_l^{j=l+\frac{1}{2}}(\varepsilon_b)+ \frac{l}{2l+1} T_l^{j=l-\frac{1}{2}}(\varepsilon_b), \tag{6}$$

so that when used in expression (4) the same absorption cross section would be obtained. Such average $T_l(\varepsilon_b)$ coefficients have been used [18]) in conjunction with expression (2).

Now according to the compound-statistical model, a compound nucleus that has been formed in a state of excitation energy U and angular momentum and parity J_c^i will de-excite by emitting one or more particles or photons, until all the energy U is dissipated. At each stage of this evaporation cascade, the rate of emission of a particle x with kinetic energy ε_x to give a product nucleus at excitation energy E_f and spin and parity J_f^k is given by [20])

$$R_x(U, J_c^i; E_f, J_f^k)dE_f = \frac{(2s_x+1)}{\pi^2\hbar^3} \mu\varepsilon_x\sigma_{inv}(J_f^k, E_f, s_x; J_c^i)\frac{\omega(E_f, J_f^k)}{\omega(U, J_c^i)} dE_f, \tag{7}$$

where s_x is the spin of particle x, μ the reduced mass and $\omega(U, J_c^i)$ and $\omega(E_f, J_f^k)$ the densities of states in the initial and final nuclei at the excitation energy, spin and parity indicated. The quantity $\sigma_{inv}(J_f^k, \varepsilon_x, s_x; J_c^i)$ is the cross section for the reaction inverse to that of the emission. This cross section should be evaluated for the particle entering through the state with E_f and J_f^k. The inverse reaction cross sections have been calculated using expressions (2) or (3) which refer to the target in the ground state. With

this approximation expressions (2) or (3) give for the inverse-reaction cross section

$$\sigma_{inv}(J_f^k, \varepsilon_x, s_x; J_c^i) = \pi \lambda^2 \frac{(2J_c^i+1)}{(2s_x+1)(2J_f^k+1)} K(J_f^k, \varepsilon_x; J_c^i), \qquad (8)$$

where $K(J_f^k, \varepsilon_x; J_c^i)$ stands for either of the sums in brackets in expression (2) or (3) with substitutions J_f^i for J_t^i, and J_c^i for J_c^k. Substitution of eq. (8) into eq. (7) yields

$$R_x(U, J_c^i; E_f, J_f^k)d\varepsilon_x = \frac{1}{\hbar} \frac{\Omega(E_f, J_f^k)}{\Omega(U, J_c^i)} K(J_f^k, \varepsilon_x; J_c^i)d\varepsilon_x, \qquad (9)$$

where $\Omega(E, J)$ is the density of levels related to the density of states by $\omega(E, J) = (2J+1)\Omega(E, J)$.

The emission function $\Gamma_x(U, J_c^i)$ in expression (1) is the emission rate given by eq. (9) integrated over ε_x and summed over J_f^k, that is

$$\Gamma_x(U, J_c^i) = [\hbar\Omega(U, J_c^i)]^{-1} \sum_{k=i}^{f} \sum_{J_f=0, \frac{1}{2}}^{J_{max}} \int_{\varepsilon=0}^{\varepsilon_{max}} \Omega(E_f, J_f^k)K(J_f^k, \varepsilon_x; J_c^i)d\varepsilon_x. \qquad (10)$$

For excitation energies below the threshold for any two-particle evaporation, expression (1) gives the desired cross section. For higher energies where multiple particle emission is possible, the one-particle cross sections can be evaluated by a proper change in the integration limits [20].

For reactions with two outgoing particles the cross section $\sigma(b, xy)$ will be given by expression (1) with the numerator of the form

$$\Gamma_{xy}(U, J_c^i) = \sum_{J_x\pi} \int_\varepsilon R_x(U, J_c^i; E_f, J_f^k) \frac{\Gamma_y(E_f, J_f^k)}{\sum_j \Gamma_j(E_f, J_f^k)} d\varepsilon_x, \qquad (11)$$

with a proper choice of the integration limits. Thus it is seen that for multiple particle evaporations, including gamma-ray competition, each additional particle corresponds to increasing the order of the integral by two degrees. Thus for one particle it is equivalent to a three-fold integral, for two particles to a five-fold integral, etc. The emission rate R_x has a rather sharp maximum for a certain choice of E_f, J_f. Therefore the most important contribution to the integral comes from a small range of values E_f, J_f near this maximum. An attempt for a direct numerical integration is very impractical because the region of maxima for R_x is not known a priori. The Monte Carlo method has two advantages; (i) it presents a simple formalism for the evaluation of cascades involving many outgoing particles, and (ii) it gives a satisfactory approximation to the integral because the sampling is properly weighted so that most of the cascades occur with R_x values near the maxima of the integrand.

In this work the gamma-ray competition in the evaporation cascade is considered in some detail. The gamma-ray emission probability is evaluated using the single-

particle amplitudes for electric or magnetic multiples of order l, thus

$$R_\gamma(U, J_c^i; \varepsilon_\gamma, J_f^k) = c_l'(J_c||\mathcal{O}||J_f)^2 \varepsilon_\gamma^{2l+1} \frac{\Omega(E_f, J_f^k)}{\Omega(U, J_c^i)}, \tag{12}$$

where c_l' is a constant depending only on the multipolarity of the emitted radiation, $(J_c||\mathcal{O}||J_f)$ the reduced matrix element for the electric or magnetic transition of multipolarity l, ε_γ the energy of the emitted radiation and $\Omega(U, J_c^i)$ and $\Omega(E_f, J_f^k)$ the densities of levels at excitation U or E_f with angular momentum J_c or J_f, respectively. The total gamma-ray width is obtained from eq. (12) by adding the contributions from the various multipoles as

$$\Gamma_\gamma(U, J_c) = \frac{1}{\Omega(U, J_c)} \sum_{l=1}^{l_{max}} c_l \sum_{J_f=J_c-l}^{J_c+l} \int_{\varepsilon_\gamma=0}^{U} \varepsilon_\gamma^{2l+1} \Omega(E_f, J_f^k) d\varepsilon_\gamma, \tag{13}$$

where the reduced matrix element in eq. (12) has been assumed constant and c_l' has been replaced by c_l to include this. For electric dipole emission from high angular momentum states, Sperber has approximated this reduced matrix element by [24]

$$(J_c||\mathcal{O}^1||J_f)^2 = \frac{R^2}{576}(2J_c+1)(2J_f+1),$$

where R is the nuclear radius. In this work the parameters c_l are adjusted to reproduce measured excitation functions for the (α, γ) reactions. This method of determining the magnitude of the gamma-ray competition is only approximate but it is believed to be satisfactory for excitations of a few MeV above threshold for the last particle. The assumption is further made that the parameter c_l is the same for all the nuclei involved in a cascade.

The transmission coefficients employed were calculated from the optical model of the nuclear potential. To this end a computer program was written to calculate elastic scattering and reaction cross sections from an optical-model nuclear potential. Some of the numerical evaluation techniques of Auerbach [25] and Melkanoff et al. [26] have been borrowed. The nuclear form factors for the potential were taken to be of the Woods-Saxon form for the real part of the nuclear potential, the Woods-Saxon derivative for volume absorption and/or Gaussian for surface absorption for the imaginary part of the nuclear potential, the Woods-Saxon derivative form for both the real and the imaginary parts of the spin-orbit interaction potential, and the form of a uniformly charged sphere inside a Coulomb nuclear radius for the Coulomb interaction. The Coulomb spin-orbit interaction term was neglected. The results of calculations of transmission coefficients with this program are in good agreement with those available in the literature, when the same set of parameters is used [27, 28].

For the evaluation of the emission functions (10) or (13), an expression for the density of levels as a function of the energy of excitation and angular momentum is needed. Of the many models that can provide such expressions the Fermi gas model

has been widely used and is also adopted in this work. The simplest version of this model which assumes the one-fermion levels to be equally spaced [29]) predicts a density of levels having the following dependence on the excitation energy:

$$\Omega(U) = \tfrac{1}{12}\pi^{\frac{1}{2}}a^{-\frac{1}{4}}(U+t)^{-5/4}\exp(2\sqrt{aU}), \qquad (14)$$

where t is the thermodynamic temperature and the parameter a is given by

$$a = \tfrac{1}{6}\pi^2[g_n(\mu_n)+g_p(\mu_p)],$$

with the equation of state

$$U = at^2 - t, \qquad (15)$$

where $g_n(\mu_n)$ and $g_p(\mu_p)$ are the single neutron and proton densities of levels at the Fermi energy, respectively. These quantities can be evaluated by considering the separate neutron and proton Fermi gases filling the entire nuclear volume. Thus, the following dependence of a on the nuclear composition is obtained:

$$a = 2(\tfrac{1}{3}\pi)^{\frac{4}{3}}\frac{mr_0^2}{\hbar^2}A\frac{Z^{\frac{1}{3}}+N^{\frac{1}{3}}}{2^{\frac{2}{3}}A^{\frac{1}{3}}}, \qquad (16)$$

or

$$a = r_0^2\frac{A^{\frac{2}{3}}(Z^{\frac{1}{3}}+N^{\frac{1}{3}})}{29.2}\,(\text{MeV}^{-1}), \qquad (17)$$

where r_0 is the nuclear radius parameter in fm and Z and N the proton and neutron number, respectively.

At high energies the exponential term in eq. (14) dominates and the previous terms may be neglected. Many authors have however used such an approximation at low energies as well.

The dependence of the density of levels on angular momentum has been discussed by Ericson [30]). Two methods have been employed in deriving this dependence. First, the distribution of the projection M of the total angular momentum on the z-axis is obtained. If the number of nucleons involved is large, this distribution tends to be Gaussian. From this Gaussian distribution, one then evaluates the density of levels as

$$\Omega(U, J) = \Omega(U, M = J) - \Omega(U, M = J+1), \qquad (18)$$

by expanding both $\Omega(U, M = J)$ and $\Omega(U, M = J+1)$ in Taylor series at $M = J+\tfrac{1}{2}$. The result is

$$\begin{aligned}
\Omega(U, J) &= \Omega(U)\frac{(2J+1)}{2\sqrt{2\pi}}\left(\frac{\hbar^2}{\mathscr{I}t}\right)^{\frac{3}{2}}\exp\left[-\frac{\hbar^2(J+\tfrac{1}{2})^2}{2\mathscr{I}t}\right] \\
&= \frac{\sqrt{2}}{48}a^{\frac{1}{4}}\left(\frac{\hbar^2}{\mathscr{I}}\right)^{\frac{3}{2}}(U+t)^{-2}(2J+1)\exp\left[2(aU)^{\frac{1}{2}}-\frac{\hbar^2(J+\tfrac{1}{2})^2}{2\mathscr{I}t}\right] \qquad (19)
\end{aligned}$$

up to the first order in the expansion. For small number of fermions or for large M, the Gaussian distribution in M does not hold. Secondly, if the nucleus has an angular momentum J, an energy $E_r = \hbar^2 J(J+1)/2\mathscr{I}$ may be taken as rotational energy not available for intrinsic excitation [31]). Consequently, the density of states is now

$$\Omega(U, J) = \Omega(U-E_r), \tag{20}$$

where $\Omega(U-E_r)$ is given by eq. (14). If E_r/U is small compared to unity, then binomial expansion of the square root in eq. (19) up to the first order yields

$$\Omega'(U, J) = \text{const} \cdot \Omega(U) \exp\left[-\frac{E_r}{t}\right], \tag{21}$$

where t was taken approximately as $(U/a)^{\frac{1}{2}}$. It should be emphasized that the Gaussian distribution on M which the derivation of eq. (19) is based becomes incorrect (earlier than the accuracy of the Taylor expansion) as M or J is increased. Similarly, the binomial expansion in the derivation of eq. (21) is a good approximation only for E_r/U small compared to unity, that is, for small values of J.

Following Grover [18]) and Sperber [17]), we define the maximum value of the angular momentum for a given excitation U via $E_r = U$, where

$$E_r \equiv \frac{\hbar^2 J(J+1)}{2\mathscr{I}}. \tag{22}$$

This means that for any given value of spin J, there is a minimum excitation energy below which no levels exist with that or higher spin. Due to the approximations involved in the derivation of eqs. (19) and (21), the density of levels is not reduced sharply enough for large values of J. To improve this situation, Lang [32]) derived a new distribution of M of the form

$$W(M) \propto \left(\frac{2\pi\mathscr{I}t}{\hbar^2}\right)^{-\frac{1}{2}} \exp\left[-\frac{\hbar^2 M^2}{2\mathscr{I}t} - \frac{\hbar^4 M^4}{(2\mathscr{I}t)^2 5g_0 t}\right].$$

A level density derived from this distribution by means of eq. (18) has an angular momentum dependence of the form

$$\Omega'(U, J) \propto \exp\left\{-\frac{\hbar^2(J+\frac{1}{2})^2}{2\mathscr{I}t}\left[1+\tfrac{1}{30}\pi^2 \frac{\hbar^2(J+\frac{1}{2})^2}{2\mathscr{I}(U+t)}\right]\right\}. \tag{23}$$

Eq. (20) has the explicit form

$$\Omega(U, J) = \frac{\sqrt{2}}{48}\left(\frac{\hbar^2}{\mathscr{I}}\right)^{\frac{3}{2}} a^{\frac{1}{4}}(U+t-E_r)^{-2}(2J+1)\exp\{2[a(U-E_r)]^{\frac{1}{2}}\}. \tag{24}$$

The binomial expansion of the square root in the exponent in expression (24) to the

second order gives

$$\Omega'(U, J) \propto \exp\left\{-\frac{\hbar^2 J(J+1)}{2\mathscr{I}t}\left[1+\frac{1}{4}\frac{\hbar^2 J(J+1)}{2\mathscr{I}U}\left(1+\frac{1}{2at}\right)\right]\right\}, \qquad (25)$$

where use was made of eq. (15). This equation is very similar to eq. (23), where a fourth-order correction to the distribution in M was included.

In the derivation of eq. (24) no simplifying approximation was made, and only a rotational energy associated with a given value of the angular momentum was defined. Thus expression (24) is a more accurate Fermi gas level density expression than that of expression (19).

The effects of pairing of protons and of neutrons in the nucleus have usually been taken into account by reduction of the excitation energy U by a condensation energy δ in the following way:

$$\begin{aligned}
\Omega_{\text{odd-mass}}(U) &= \Omega_{\text{even}}(U+\delta), & U &> \delta, \\
\Omega_{\text{doubly odd}}(U) &= \Omega_{\text{even}}(U+2\delta), & U &> 2\delta.
\end{aligned} \qquad (26)$$

The neutron or proton condensation energies δ_n or δ_p can be treated separately, however, in an obvious manner. Furthermore, these condensation energies are equated to the pairing energies, as calculated by various authors [33].

The pairing effects are more naturally introduced, however, via the superconductor model for the nucleus as applied by Lang [34] and Vonach et al. [35] for the derivation of an expression for the density of levels in a nucleus.

3. Calculations and results

As was mentioned earlier, the Monte Carlo technique was employed in calculations of excitation functions and particle-evaporation spectra. In this technique it is assumed that the reaction proceeds via a cascade of evaporations.

First, for a specified bombarding energy, the formation of a compound nucleus is considered with a fixed excitation energy U, but with angular momentum J_c given by either expression (2) or (3) with a maximum value set by expression (22). The weighted choice of J_c is based on drawing two random numbers; the first selects J_c and the second determines if this value will be accepted (if $\sigma^b_{\text{comp}}(U, J_c) \geqq \xi_2$) or rejected (if $\sigma^b_{\text{comp}}(U, J_c) < \xi_2$).

Secondly, the de-excitation of the compound nucleus with the given U and chosen J_c involves the emission of a number of particles or gamma rays until a stable, final nucleus is reached. The evaporation of each particle is treated separately, implying equilibrium between evaporations. At each step of the cascade $\Gamma_x(U, J_c)$ is evaluated for a neutron, proton and ^{4}He particle via eq. (10) or for gamma rays via eq. (13). The sum of these emission functions is normalized to unity, and the particle to be emitted is selected by a random number between 0 and 1.

Next, the parameters involved in the emission of the selected particle are determined by choice of three random numbers. The first random number selects the parity change, the second determines the spin of the final state J_f which defines $E_r = \hbar^2 J_f (J_f + 1)/2\mathscr{I}$ not available for intrinsic excitation. The third number determines whether an emission with kinetic energy $\varepsilon_x = \xi_3 \varepsilon_{max}$ is to be accepted (if $0 < \xi_3 < 1 - E_r/\varepsilon_{max}$) or rejected (if $\varepsilon_x < 0$ or $\xi_3 > 1 - E_r/\varepsilon_{max}$). Here ε_{max} is equal to $(U - B_x)$, where B_x is the separation energy of the particle x from the emitting nucleus. The choice of (J_f^k, ε_x) has to be weighted according to eq. (9). The emission rate $R_x(U, J_c^i; E_f, J_f^k)$ is evaluated and a fourth random number determines if the above choice (J_f^k, ε_x) is to be accepted (if $R_x > \xi_4$) or rejected (if $R_x \leqq \xi_4$). A successful emission with (J_f^k, ε_x) is followed by evaporation of a second particle from a compound nucleus with $U' = U - B_x - \varepsilon_x$ and $J_c^{i'} = J_f^k$ in an identical manner. This is repeated until no further emission is energetically possible at which point the cascade ends to a specified product nucleus.

For each projectile energy a large number (usually 500–2 000) of cascades is computed, and the results are summarized to provide the following information: the total number of particles of each kind that were emitted, the energy spectra of these particles, the number of cascades that led to the various final product nuclei, the spin distributions in the initial and final nucleus (after the emission of the last particle and preceding the final gamma cascade) and the details of excitation energy and spin distributions at intermediate stages of the evaporation cascade. The cross section for the formation of a particular product nucleus is evaluated as the product of the total reaction cross section for compound nucleus formation at that projectile energy and the fraction of the cascades that led to the nucleus in question. A complete excitation function is then obtained by repeating this entire process at a series of projectile energies.

The computer program "ROULETTE", that was written for the Washington University IBM 7072 computer, was limited by the core size to a maximum of three consecutive emissions of neutrons or of protons. The calculation was limited to the emission of neutrons, protons, ^{4}He particles and gamma rays, which is believed to be satisfactory if the initial excitation does not exceed 40 MeV. Some further simplifying approximations had to be made to make the computation practical.

The formalism as presented earlier included the dependence of the emission probability on parity changes. For high excitation energies the number of positive or negative parity states may be assumed to be the same so that parity effects enter only through the capture or inverse reaction cross section as in expressions (2) or (3). Two typical cases for capture of a ^{4}He particle need to be discussed; (i) for target nuclides with $J_t^\pi = 0^+$, the capture cross section evaluated via expression (2) gives J_c^- if J_c is odd and J_c^+ if J_c is even. In this case only one l contributes per J-value. This is illustrated in fig. 1 where the capture cross section of ^{4}He ions by ^{92}Mo is given for two projectile energies; (ii) for target nuclides with spin $\frac{1}{2}$ or higher, two or more transmission coefficients with different l-values contribute to each J_c. It is easy to see that
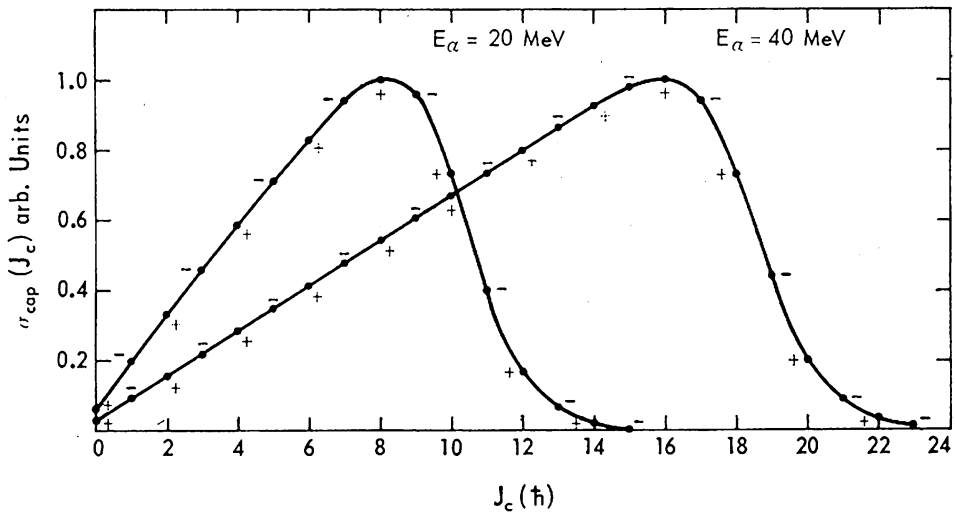
Fig. 1. Total reaction cross section for the formation of the compound nucleus ^{96}Ru by ^{92}Mo+^{4}He ions. The relative population of states with definite spin and parity is given for two projectile energies.

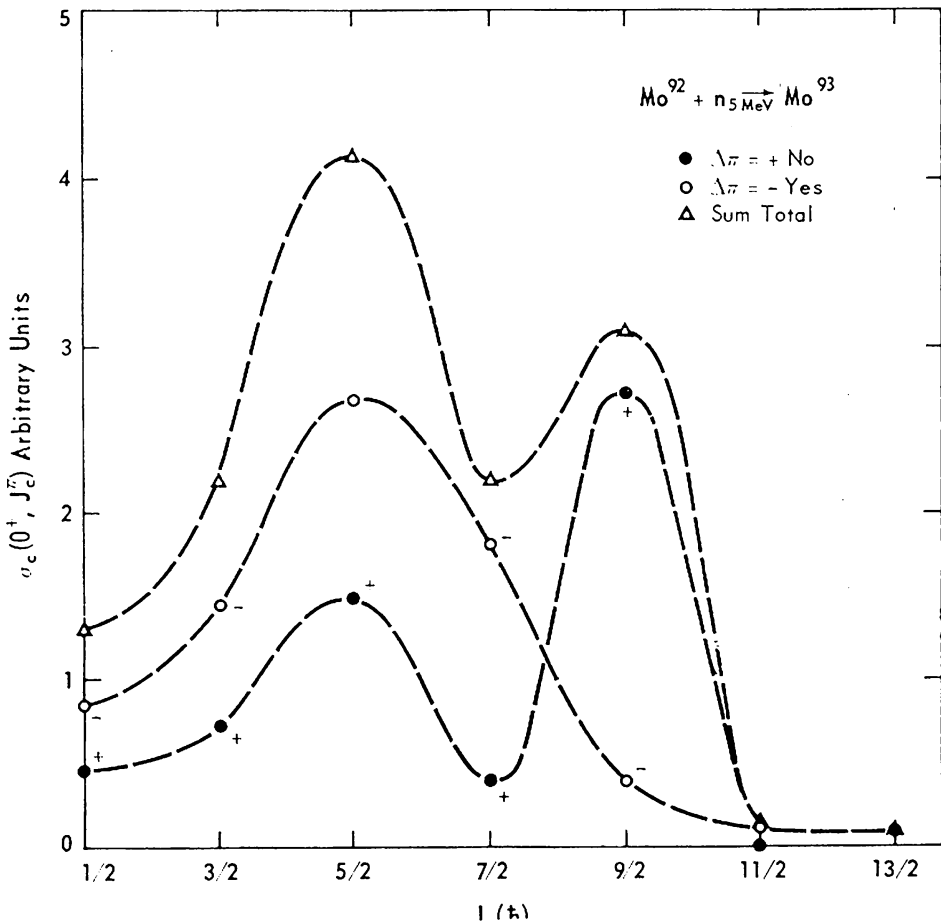Fig. 2. Total reaction cross section for the formation of the compound nucleus ^{93}Mo by ^{92}Mo+$n_{5\,MeV}$. The relative population of states with definite parity change is shown as a function of their spin. Populations of the same parity are connected with dashed curves.

the low J_c part of the capture cross section contains an equal number of states of both parities, while the high J_c part will show some fluctuations with J_c. For higher target spins these fluctuations are appreciably smaller, and in all cases of interest averages over a small range of J_c values yield smooth and equal distribution of states of both parities.

For neutron- or proton-induced reactions or in evaporation of such particles, parity selection rules may be of importance. This arises from the inclusion of the spin-orbit interaction term in the optical potential thus yielding transmission coefficients $T_l^{j=l+\frac{1}{2}}(\varepsilon)$ and $T_l^{j=l-\frac{1}{2}}(\varepsilon)$ which may differ appreciably in magnitude. As an illustration of this, consider the cross section for the capture of 5 MeV neutrons by a target nucleus with $A = 100$ and $J_t^\pi = 0^+$ as calculated via expression (3) and shown in fig. 2. It is seen that, for example, the most probable spins of states with or without parity change differ by $2\hbar$ units. Thus, an uneven population would be expected for states of opposite parities for a given angular momentum in compound nuclei formed from low-spin targets. This effect will influence the outcome of de-excitation by proton or neutron emission. For high-spin targets, this effect averages out because of the larger number of l-values contributing to each J_c value.

In calculations on ^{4}He-induced reactions the parity selection rules have been neglected.

The second approximation involves the transmission coefficients used. A table of transmission coefficients for each type of particle, each l-value needed and a set of energies between zero and the maximum particle energy is stored in the memory. For intermediate energies a logarithmic interpolation is employed. For an exact calculation a table, of $T_l(\varepsilon)$ values is needed for each emitting nucleide. Core memory size limits the number of $T_l(\varepsilon)$ values that can be stored. Since the transmission coefficients change on the average rather slowly with nuclear composition (over a range of a few mass numbers), averaging over the latter is considered a satisfactory approximation. Thus for proton or neutron emission an average nucleus with $(Z-1, A-2)$ was assumed for the evaluation of the transmission coefficients, where (Z, A) is the original compound nucleus. For alpha-particle emission, however, the average nucleus was $(Z-2, A-4)$. Under these assumptions the emission rates $R_x(U, J_c; E_f, J_f)$ and the total emission functions $\Gamma_x(U, J_c)$ were evaluated for different "average" residual nuclei with changes of ± 2 charge units and ± 4 mass units. Such a variation resulted in a variation of a few percent in the neutron emission function $\Gamma_n(U, J_c)$ and a maximum variation of 15 % for the proton-emission function $\Gamma_p(U, J_c)$. The alpha-emission function $\Gamma_\alpha(U, J_c)$ varies more strongly than this with Z or A. Thus, a variation of two charge units results in a change of about 50 % in $\Gamma_\alpha(U, J_c)$. However, these variations in average composition are much larger than those occurring in the course of a calculation where only a few particles are actually evaporated. Therefore, the errors introduced into the calculated cross sections are probably small compared with the errors in these quantities measured experimentally. In all the results that will follow the level density parameter a was calculated according to eq. (17) with $r_0 = 1.22$ fm, and the moment of inertia was taken as that of a rigid sphere.
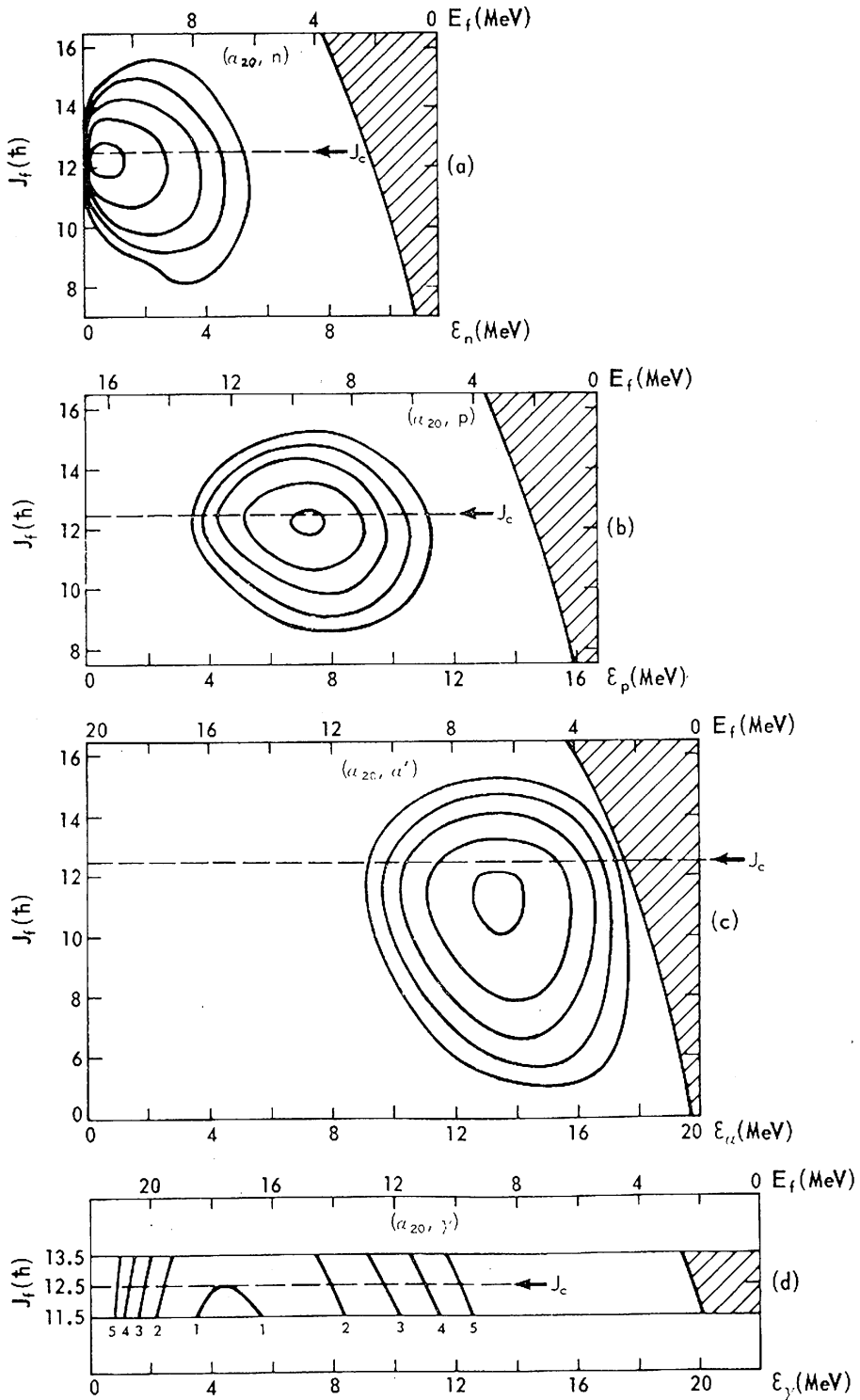
Fig. 3. The emission rates $R_x(U, J_c; \varepsilon, J_f)$ for neutrons, protons, alpha particles and gamma rays are shown in (a), (b), (c) and (d), respectively. The compound nucleus in ^{111}In with $U = 21.98$ MeV and $J_c = 12.5 \hbar$ units. The shaded area indicates the region of no states and is bounded by the rotational energy cut-off E_r and the threshold. The lower scale for the abscissa gives the kinetic energy of the outgoing particle and the upper scale the residual excitation energy in MeV. The highest probability is that of the inner contour, with a factor of two between adjacent isoprobability contours. The dashed horizontal line indicates the spin J_c of the emitting state.

The importance of the angular momentum effects on the emission rates can be best illustrated in a typical example, the system ^{107}Ag(α, x) for two alpha energies 10 and 20 MeV. Figs. 3a–d give a plot of R_x as evaluated by eq. (9) in a contour form. Here
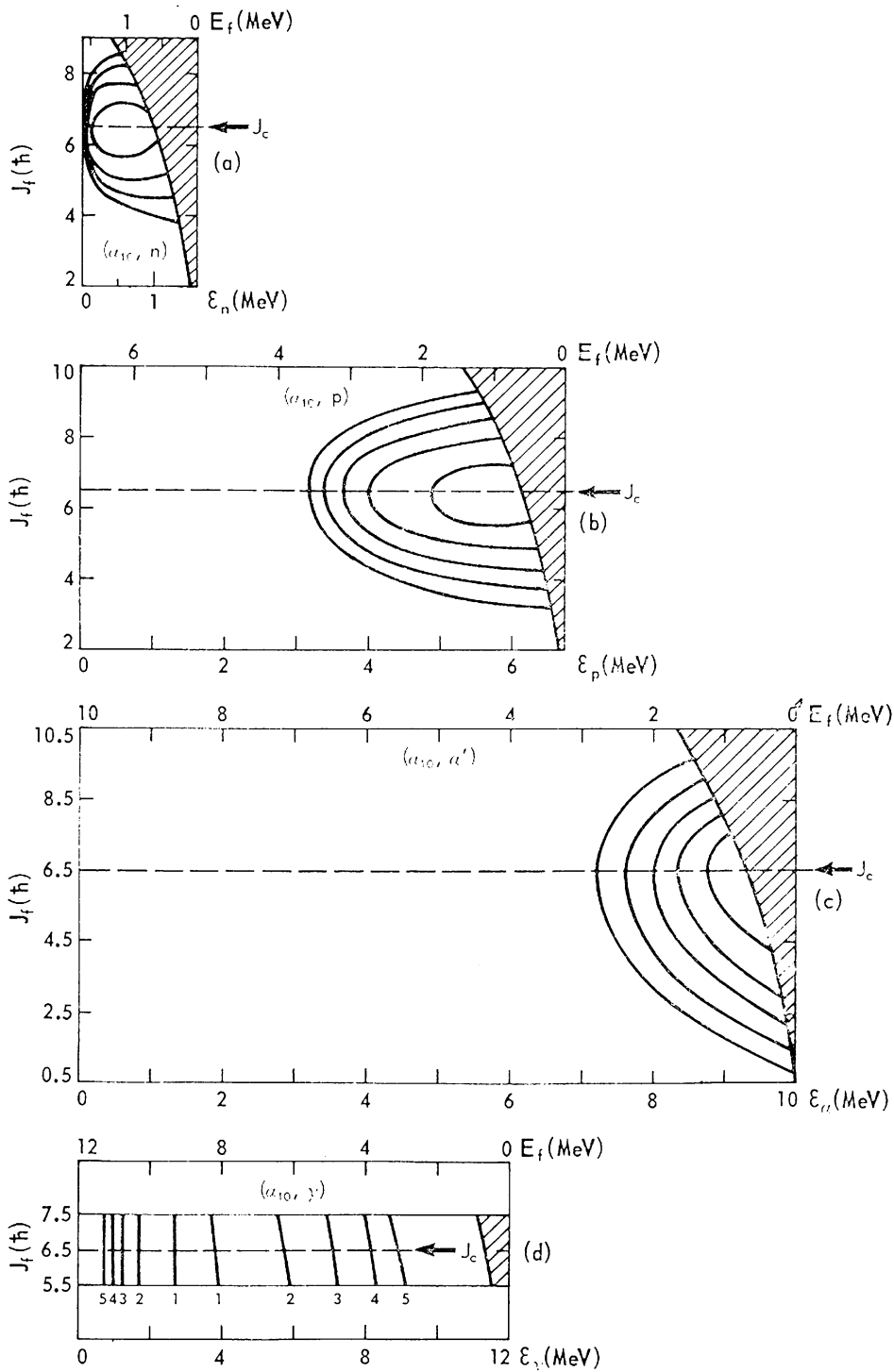

Fig. 4. Emission rates $R_x(U, J_c; \varepsilon, J_f)$ as in fig. 3 with $U = 11.98$ MeV and $J_c = 6.5\ \hbar$ units.

the compound nucleus is ^{111}In at 21.98 MeV excitation energy and spin J_c of $12.5\hbar$ units. The abscissa in each case is the kinetic energy of the evaporated particle or the excitation energy of the residual nucleus (upper scale). The ordinate is the angular momentum of the residual nucleus J_f. The emission rate is given in isoprobability contours with a decrease of a factor of two between contours going outwards. The scale is arbitrary. Here the variables J_f and E_r are shown as continuous for clarity. The end line to the right corresponds to the maximum available particle energy and the shaded area to those combinations of energy and angular momentum for which
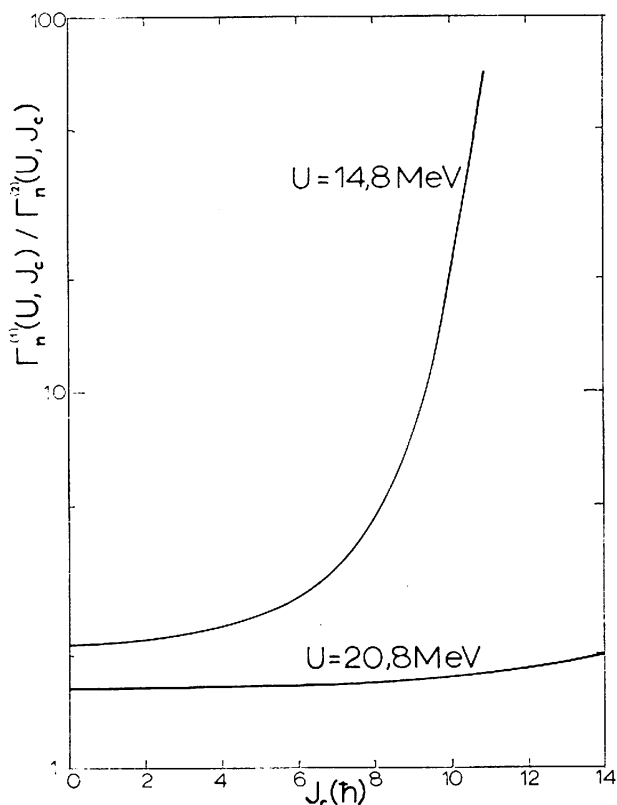
Fig. 5. The effect of uncertainties in the neutron separation energies on the total neutron emission probability. This is indicated as the ratio of two values for $\Gamma_n(U, J_c)$ evaluated for two neutron separation energies of 11.31 and 12.01 MeV in the ^{68}Ge compound nucleus as a function of J_c for two excitation energies U of 14.8 and 20.8 MeV.

states cannot exist, as discussed earlier. In this region beyond the rotational-energy cut-off, the level density was set to zero. It is seen from fig. 3 that on the average there is a lowering in the spin of about $1\hbar$ unit for the emission of one neutron or proton and of about $2\hbar$ units for the emission of an alpha particle.

Figs. 4a–d give the emission functions R_x for the same compound nucleus at 11.85 MeV excitation and with J_c of $6.5\hbar$ units. The effect of the rotational-energy cut-off is now clearly seen. The gamma-ray emission rate R_γ, however, is not influenced appreciably by this effect. Thus the particle to gamma-ray emission rate Γ_x/Γ_γ should be decreasing with increasing J_c. In fig. 4 it is seen that a change in the separation ener-

gy for any of the outgoing particles affects the threshold for that reaction. The rotational energy, however, is not affected by this, so that one expects uncertainties in the separation energies to be strongly reflected on the calculated value for the emission function $\Gamma_x(U, J_c)$. This effect is more clearly illustrated in fig. 5, where the ratio of the neutron emission function for two assumed values 11.31 and 12.01 MeV for the neutron separation energy is plotted as a function of J_c. The compound nucleus is ^{68}Ge produced by bombardment of ^{64}Zn with ^{4}He ions; this reaction is analysed in this work. It is seen that for low excitations there is a strong dependence on J_c. Such
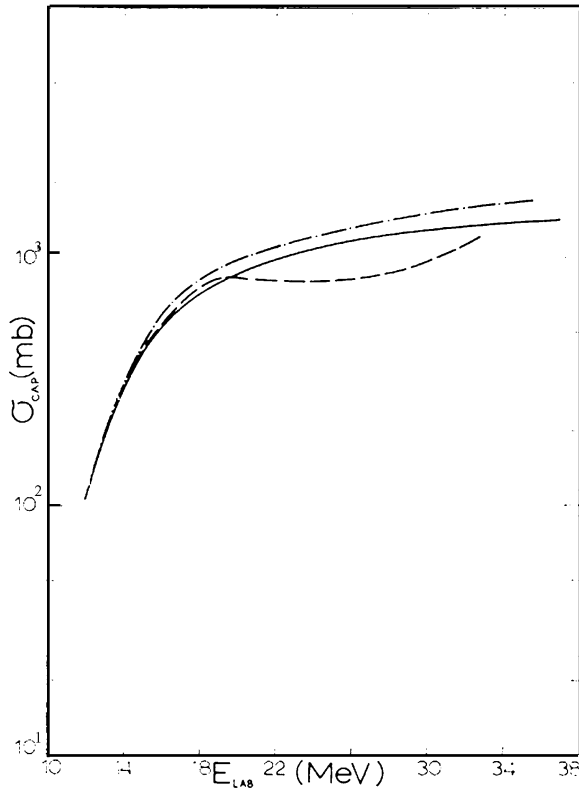

Fig. 6. Total reaction cross section for ^{64}Zn+^{4}He ions. The dashed curve represents the sum of experimentally measured cross sections. The solid line gives the reaction cross section calculated via the optical model. The dot-and-dash curve gives the experimental total reaction cross section corrected for the missing fraction due to the non-measured $(\alpha, 2p)$, (α, α') and $(\alpha, \alpha'p)$ reactions.

an artifact can introduce an erroneous dependence on J_c whenever separation energies are used which differ from the true ones.

The effect of uncertainties in the pairing term δ on the J_c dependence of the neutron emission function was also investigated. In this work the pairing energy correction to the density of levels was introduced in such a way that for excitations $(U-E_r)$ higher than 2 MeV above δ, eq. (24) is used for the density of levels. For the case $0 < (U-E_r) < (\delta+2)$ MeV the following approximation is made. The density of levels and its logarithmic slope are evaluated at the arbitrary energy of $(\delta+2)$ MeV and for each J-value a logarithmic extrapolation is made down to the true energy which may be

below the pairing energy. For the present purposes it is believed that this approxima-
tion is appropriate. When U is equal to the rotational energy, the density of levels is
set equal to zero. It was thus found that the pairing correction δ did not affect the
J-dependence of the emission function but only its magnitude. Therefore, the pairing
energy terms δ can be adjusted within the limits set by experimental uncertainties in
the nucleidic masses in order to improve the fit of the calculated cross sections with
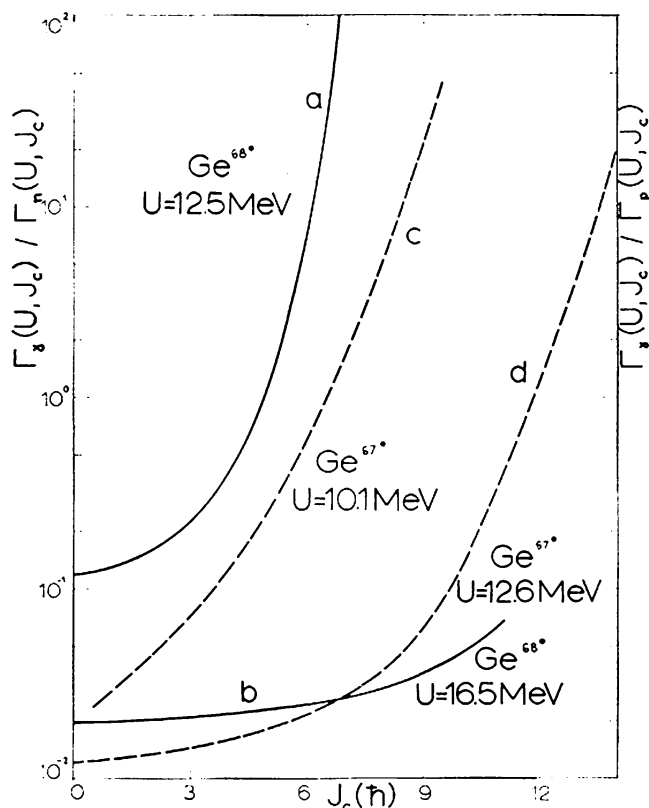experimental excitation functions.

Fig. 7. Gamma-ray emission versus neutron and proton emission in the de-excitation of ^{68}Ge and
^{67}Ge compound nuclei as a function of angular momentum. Curves a and b refer to the ^{68}Ge com-
pound nucleus and give the ratio $\Gamma_\gamma(U, J_c)/\Gamma_n(U, J_c)$ for two excitation energies of $U = 12.5$ and
16.5 MeV, respectively. Curves c and d refer to the ^{67}Ge compound nucleus and give the ratio
$\Gamma_\gamma(U, J_c)/\Gamma_p(U, J_c)$ for two excitation energies of $U = 10.1$ and 12.6 MeV, respectively.

The calculated total reaction cross section using optical-model transmission coeffi-
cients is shown in fig. 6 (solid line). The dashed line corresponds to the sum of the
measured cross sections from the data of Porile [6]). The dot-and-dash curve gives the
experimental total reaction cross section corrected for the fraction due to the radio-
chemically inaccessible $(\alpha, 2p)$, (α, α') and $(\alpha, \alpha'p)$ reactions, as estimated in the
present calculation.

The dependence on the angular momentum J_c of the competition for de-excitation
by gamma-ray emission versus particle emission is best illustrated in a plot of the ratio
of the emission function $\Gamma_\gamma(U, J_c)/\Gamma_n(U, J_c)$ or $\Gamma_\gamma(U, J_c)/\Gamma_p(U, J_c)$. In this work the

magnitude of $\Gamma_\gamma(U, J_c)$ is determined by the value of the assumed parameter c_l in eq. (13). For electric dipole emission the value $2 \times 10^{-5}\ \mathrm{erg}^{-4}\ \mathrm{sec}^{-1}$ for c_1 reproduces the measured cross section for the $^{64}\mathrm{Zn}(\alpha, \gamma)$ reaction. With this value for c_1, the ratios of the gamma to neutron and to proton emission functions for $^{68}\mathrm{Ge}$ and $^{67}\mathrm{Ge}$ compound nuclei are given for two excitation energies in each case as a function of the angular momentum of the compound state (see fig. 7). It is clearly seen that gamma competition becomes important with increasing J_c and the effect is very pronounced
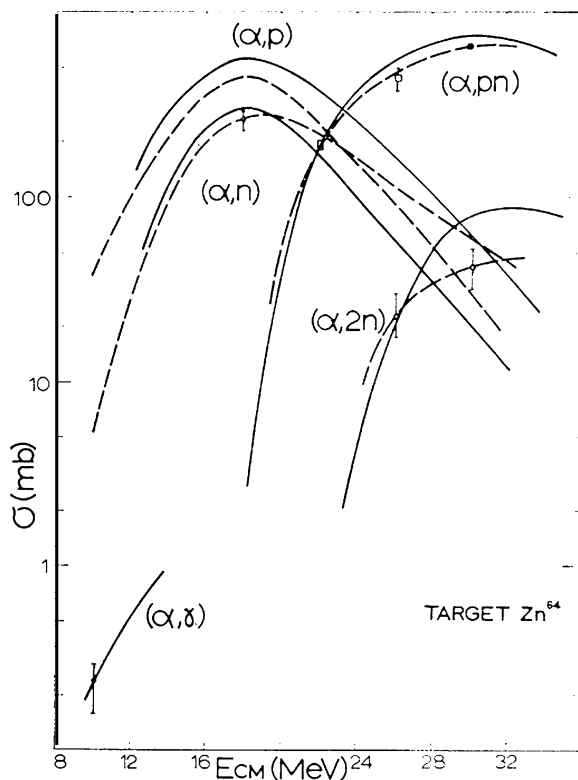

Fig. 8. Excitation functions of reactions induced by ^{4}He ions on ^{64}Zn. The solid lines represent the best empirical curves drawn through the data points of ref. [6]). The dashed curves represent the calculated excitation functions normalized to the dot-and-dash curve of fig. 6.

for excitation energies not exceeding a few MeV above the threshold for the emission of that particle. The sharp rise in the gamma-ray emission relative to that for particle emission is clearly understood in terms of the plots given in fig. 4. The neutron emission function $\Gamma_n(U, J_c)$ decreases sharply with increasing J_c because emissions carrying small values of orbital angular momentum are contributing, so that the rotational-energy cut-off reduces $\Gamma_n(U, J_c)$ considerably. The gamma-emission function, however, is insensitive to changes in J_c (fig. 4d).

In fig. 8 the solid lines represent the best curves drawn through the excitation function data of Porile [6]) for the reactions (α, p), (α, n), (α, γ), (α, pn) and $(\alpha, 2n)$ on ^{64}Zn. The dashed curves represent the calculated cross sections normalized to the corrected

experimental total reaction cross section. Bars have been drawn on some of the calculated points indicating deviations due to the random number choice and correspond to the square root of the number of events leading to that particular reaction. It is believed that this is overestimating the standard deviation, because repeated calculations with different random numbers have yielded statistical deviations significantly smaller than those indicated by the bars.

The values of the particle-separation energies used are those of König et al. [36]) with some slight changes by at most one standard deviation. No attempt has been
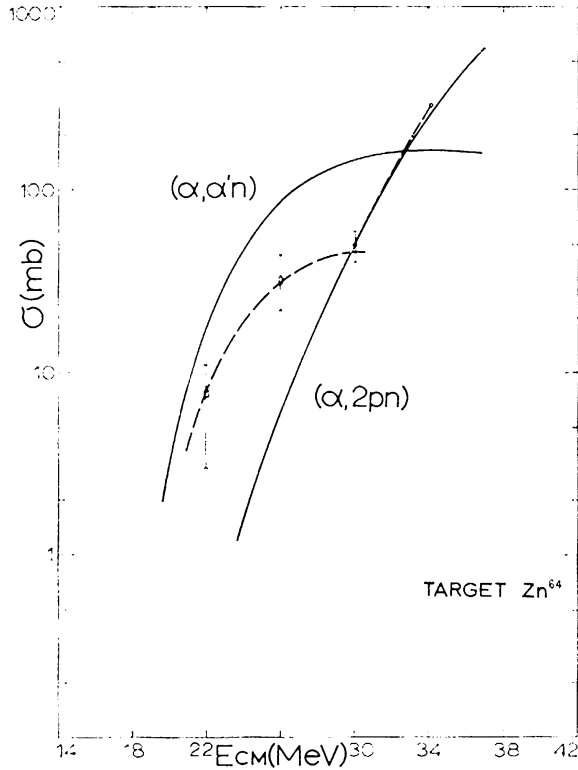

Fig. 9. Excitation functions for the $(\alpha, \alpha'n)$ and $(\alpha, 2pn)$ reactions in ^{64}Zn targets. The solid lines represent the experimental data and the dashed curves the calculated cross sections. These have been presented in a different plot for purposes of clarity.

made to find the optimum set of adjustments on the separation energies that will provide the best agreement with the experimental excitation functions. The pairing terms δ of Cameron [33]) were used but δ_z for $Z = 32$ had to be reduced by ≈ 0.4 MeV in order to obtain a reasonable fit with the excitation function data. Again no attempt to find the best adjusted δ-values was made. The level-density parameter a was evaluated according to eq. (17) with $r_0 = 1.22$ fm, and rigid-body moments of inertia were employed throughout. The fit to the data may be considered satisfactory. It is noteworthy, however, that the high-energy tail for the (α, p) has the correct slope while that for the (α, n) has a higher slope than the experimental curve. The importance of the gamma-ray competition against proton and neutron emission is reflected in the

ratio of the cross section for the $(\alpha, p)/(\alpha, pn)$ which rises with increasing c_1. The ratio of the cross sections for $(\alpha, n)/(\alpha, 2n)$, however, is not influenced in this particular case by the assumed gamma-ray emission strength. This is so because in the product of the (α, n) reaction ^{67}Ge, the probability of emitting a proton from states of a few MeV above the second neutron threshold is about 10–20 times larger than that of emitting a neutron.

The calculated cross sections for the $(\alpha, 2pn)$ and $(\alpha, \alpha'n)$ reactions (dashed lines) are shown in fig. 9 together with the experimental curves (solid lines). Finally, fig. 10
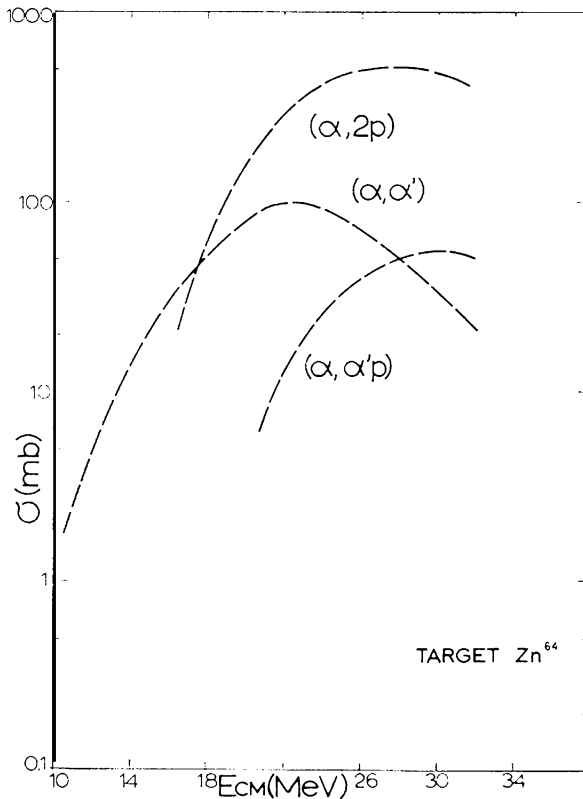

Fig. 10. Calculated excitation functions for the radio-chemically non-measurable reactions ^{64}Zn$(\alpha, 2p)^{66}$Zn, ^{64}Zn$(\alpha, \alpha')^{64}$Zn and ^{64}Zn$(\alpha, \alpha'p)^{63}$Cu.

gives the calculated cross sections for the radiochemically, non-measurable reaction products $(\alpha, 2p)$, (α, α') and $(\alpha, \alpha'p)$ on ^{64}Zn. From the last figure it is seen that the reaction $(\alpha, 2p)$ is the main competitor of the (α, pn) with comparable cross sections.

In conclusion it must be said that in this reaction system satisfactory agreement of theory and experiment is obtained if angular momentum is properly included in the formalism. It should be noted that this agreement was obtained using the level-density parameter a and the moment of inertia as predicted by the Fermi gas model for excitation energy of at least a few MeV.

A systematic study of the dependence of the calculated excitation functions on the model parameters for another reaction system is presented in the following paper.

Appendix

CAPTURE CROSS SECTIONS IN THE j-j COUPLING SCHEME

In the following, the notation used in eq. (2) will be used and the derivation will be limited to particles of spin $s_x = \frac{1}{2}$. Particles of unit spin are treated in an analogous fashion. First, l and s_x are coupled to obtain $j^{\pm} = l \pm \frac{1}{2}$. Then, the states $|j^{\pm}m\rangle$ are coupled with the states $|J_t m_{j_t}\rangle$ to obtain the states $|J_c M_{j_c}\rangle$. In the language of partial wave expansion of the ingoing particle, the cross section for this reaction can be written as

$$
\sigma(J_t, j, m_{j_t}; J_c, M_{j_c}) = \pi \lambdabar^2 [(l+1) T_l^{j^+}(\varepsilon)
$$
$$
\times |\langle J_t j^+ m_{j_t} m_{j+} | J_t j^+ J_c M_{j_c}\rangle|^2 + l T_l^{j^-}(\varepsilon) |\langle J_t j^- m_{j_t} m_{j-} | J_t j^- J_c M_{j_c}\rangle|^2], \quad (A.1)
$$

where $T_l^{j^{\pm}}(\varepsilon)$ are the transmission coefficients for the lth partial wave of the incoming particle with intrinsic spin parallel or anti-parallel to the orbital angular momentum transferred into the system and $\langle J_t j m_{j_t} m_j | J_t j J_c M_{j_c}\rangle$ the Clebsch-Gordan coefficient connecting the corresponding angular momenta. Averaging over the initial states m_{j_t}, m_j and summing over the final states M_{j_c} gives

$$
\sigma(J_t, j; J) = \pi \lambdabar^2 \frac{1}{(2s_x+1)(2J_t+1)} [T_l^{j^+}(\varepsilon) + T_l^{j^-}(\varepsilon)]
$$
$$
\times \sum_{M_{j_c}} \sum_{m_j} \sum_{m_{j_t}} |\langle J_t j m_{j_t} m_j | J_t j J_c M_{j_c}\rangle|^2. \quad (A.2)
$$

Use of the properties of the Clebsch-Gordan coefficients in eq. (A.2) yields

$$
\sigma(J_t, j; J_c) = \pi \lambdabar^2 \frac{(2J_c+1)}{(2J_t+1)(2s_x+1)} [T_l^{j^+}(\varepsilon) + T_l^{j^-}(\varepsilon)]. \quad (A.3)
$$

Finally, summing over all the values of l that satisfy the triangular condition

$J_t - j \leqq J_c \leqq J_t + j$ for $j = l + \frac{1}{2}$ and for $j = l - \frac{1}{2}$ yields

$$\sigma(J_t, s_x; J_c) = \pi \lambda^2 \frac{(2J_c + 1)}{(2J_t + 1)(2s_x + 1)}$$

$$\times \left[\sum_{l = |J_c - J_t \pm \frac{1}{2}|}^{J_c + J_t + \frac{1}{2}} T_l^{j = l - \frac{1}{2}}(\varepsilon) + \sum_{l = |J_c - J_t \mp \frac{1}{2}| \{ \begin{smallmatrix} \text{for } J_c > J_t \\ \text{for } J_c < J_t \end{smallmatrix}}^{J_c + J_t - \frac{1}{2}} T_l^{j = l + \frac{1}{2}}(\varepsilon) \right], \quad (A.4)$$

which is identical to eq. (3).

For particles of spin $s_x = 1$ the corresponding equation is

$$\sigma(J_t, s_x; J_c) = \pi \lambda^2 \frac{(2J_c + 1)}{(2J_t + 1)(2s_x + 1)} \left[\sum_{l = |J_c - J_t \mp 1| \neq 0}^{J_c + J_t - 1} T_l^{j = l + 1}(\varepsilon) \right.$$

$$\left. + \sum_{l = |J_c - J_t|}^{J_c + J_t} T_l^{j = l}(\varepsilon) + \sum_{\substack{l = |J_c - J_t \pm 1| \{ \begin{smallmatrix} \text{for } J_c > J_t \\ \text{for } J_c < J_t \end{smallmatrix} \\ \neq 0}}^{J_c + J_t + 1} T_l^{j = l - 1} \right]. \quad (A.5)$$

References

1) V. F. Weisskopf, Phys. Rev. **52** (1937) 294
2) H. A. Bethe, Revs. Mod. Phys. **9** (1937) 69
3) J. Blatt and V. F. Weisskopf, Theoretical nuclear physics (John Wiley, New York, 1952)
4) K. J. Le Couteur, in Nuclear reactions, ed. by P. M. Endt and M. Demeur (North-Holland Publishing Co., Amsterdam, 1959)
5) T. Ericson, Advan. Phys. **9** (1960) 425
6) N. T. Porile, Phys. Rev. **115** (1959) 939
7) I. Dostrovsky, Z. Fraenkel and G. Friedlander, Phys. Rev. **116** (1959) 683
8) F. S. Houck and J. M. Miller, Phys. Rev. **123** (1961) 231
9) R. L. Hahn and J. M. Miller, Phys. Rev. **124** (1961) 1879
10) L. F. Hansen and R. D. Albert, Phys. Rev. **128** (1962) 291
11) K. Chen, Ph.D. thesis, Columbia University (1962)
12) S. Fukushima, S. Hayashi, S. Kume, H. Ikamura, K. Otozai, K. Sakamoto and Y. Yashizawa, Nuclear Physics **41** (1963) 275
13) C. Hurwitz, S. J. Spencer, R. A. Esterlund, B. D. Pate and J. B. Reynolds, Nuclear Physics **54** (1964) 65
14) T. D. Thomas, Nuclear Physics **53** (1964) 558, 577
15) C. T. Bishop, J. R. Huizenga and J. P. Hummel, Phys. Rev. **135** (1964) B401
16) R. Vandenbosch, L. Haskin and J. C. Norman, Phys. Rev. **137** (1965) B1134
17) D. Sperber, Ph.D. thesis, Princeton University (1960); Phys. Rev. **141** (1966) 927
18) J. R. Grover, Phys. Rev. **127** (1962) 2142
19) J. R. Grover and R. J. Nagle, Phys. Rev. **134** (1964) B1248
20) R. A. Esterlund and B. D. Pate, Nuclear Physics **69** (1965) 401
21) M. Blann, F. M. Lanzafame and R. A. Piscitelli, Phys. Rev. **133** (1964) B700
22) M. Blann, Phys. Rev. **133** (1964) B707
23) M. Blann and G. Merkel, Phys. Rev. **137** (1965) B367
24) D. Sperber, Phys. Rev. **142** (1966) 578
25) E. H. Auerbach, Abacus-2, Brookhaven National Laboratory, unpublished
26) M. A. Melkanoff, D. S. Saxon, J. S. Nodvik and D. G. Cantor, A Fortran program for elastic scattering analyses with the nuclear optical model (University of California Press, Berkeley, 1961)
27) E. H. Auerbach and F. G. Perey, Brookhaven National Laboratory Report BNL 765 (T-286)

28) J. R. Huizenga and G. Igo, Nuclear Physics **29** (1962) 462
29) J. M. Lang and K. J. Le Couteur, Proc. Phys. Soc. **67A** (1954) 586
30) T. Ericson, Phil. Mag. Suppl. **9** (1960) 425
31) D. W. Lang, Nuclear Physics **77** (1966) 545
32) D. W. Lang, Conf. on Reactions of complex nuclei, Asilomar, California, to be published and private communication (1964)
33) A. G. W. Cameron, Can. J. Phys. **36** (1958);
    P. A. Seeger, Nuclear Physics **25** (1961) 1;
    M. Hillman, private communication (1965)
34) D. W. Lang, Nuclear Physics **42** (1963) 353
35) H. K. Vonach, R. Vandenbosch and J. R. Huizenga, Nuclear Physics **60** (1964) 70
36) L. A. König, J. H. E. Mattauch and A. H. Wapstra, Nuclear Physics **31** (1962) 18